Chapter 4

F_L Structure Function from Gluon Distribution Function Using Taylor Expansion Method at Small-x

In this chapter, we have presented the relation between the F_L structure function and the gluon distribution function up to next-to-next-to-leading order analysis at small-x using Taylor expansion method. We use the Altarelli-Martinelli equation in our analysis to obtain the evolution of F_L structure function at small-x. The obtained theoretical results are compared with H1 [1–5], ZEUS [6] data, results of DL [7] model, results predicted by MSTW08 [8], CT10 [9, 10], ABM11 [11] and NNPDF2.3 [12, 13] parameterizations and results obtained by other authors.

4.1 Theory

In pQCD, the Altarelli-Martinelli equation for longitudinal structure function $F_L(x, Q^2)$ of proton in terms of co-efficient function is given by [14, 15]

$$x^{-1}F_L = C_{L,ns} \otimes q_{ns} + < e^2 > (C_{L,s} \otimes q_s + C_{L,g} \otimes g). \tag{4.1}$$

Here q_{ns}, q_s and g are the flavour non singlet, flavour singlet and gluon distribution function, $< e^2 >= \frac{5}{18}$ is the average squared charge for N_f (number of active light flavours) and the symbol $\otimes$ represents the standard Mellin convolution. $C_{L,a}(a = ns, s, g)$'s are the co-efficient functions which can be written by the perturbative expansion as follows [15]

$$C_{L,a}(\alpha_s, x) = \sum_{n=1} \Big(\frac{\alpha_s}{4\pi}\Big)^n C^n_{L,a}(x), \tag{4.2}$$

where n denotes the order in running coupling constant $\alpha_s(Q^2)$ [16] and the expression of α_s is mentioned in section 2.1 of chapter 2.

At small values of x ($x \leq 10^{-3}$) the gluon contribution to the F_L structure function dominates over the flavour singlet and non-singlet contribution [17]. Now the Altarelli Martinelli equation for gluon dominating F_L structure function is given by

$$F^g_L(x, Q^2) =< e^2 > \int_x^1 \frac{dw}{w} C_{L,g}(w, Q^2) G\Big(\frac{x}{w}, Q^2\Big). \tag{4.3}$$

Here $C_{L,g}(w, Q^2)$ is the gluon co-efficient function for F_L known perturbatively up to first few orders in running coupling constant $\alpha_s(Q^2)$ and can be written as

$$C_{L,g}(w, Q^2) = \frac{\alpha_s(Q^2)}{4\pi} C^1_{L,g}(w) + \Big(\frac{\alpha_s(Q^2)}{4\pi}\Big)^2 C^2_{L,g}(w) + \Big(\frac{\alpha_s(Q^2)}{4\pi}\Big)^3 C^3_{L,g}(w), \tag{4.4}$$

where $C^1_{L,g}(w)$, $C^2_{L,g}(w)$ and $C^3_{L,g}(w)$ are the gluon co-efficient functions for F_L in LO, NLO and NNLO respectively [15, 18, 19]. The analytical expression of the gluon co-efficient function for F_L are defined in the Appendix A.

At small values of x we can rewrite the equation (4.3) by substituting $w = 1 - z$ as

$$F^g_L(x, Q^2) =< e^2 > \int_0^{1-x} \frac{dz}{1-z} C_{L,g}(1-z, Q^2) G\Big(\frac{x}{1-z}, Q^2\Big), \tag{4.5}$$

where F^g_L is derived from the integrated gluon distribution function $G(x, Q^2)$. An approximate relationship between F^g_L and gluon distribution can be obtained from the expansion of $G\Big(\frac{x}{1-z}, Q^2\Big)$ around a particular choice of point of expansion. Since $x < w < 1$, we have $0 < z < 1 - x$; so the series $\frac{x}{w} = \frac{x}{1-z}$ is convergent for $|z| < 1$. So, we can take the point of expansion z as any value between $0 \leq z < 1$.

Using the Taylor expansion method for the gluon distribution function at an arbitrary point $z = \frac{1}{2}$, and neglecting the higher order terms at small-x, $G\Big(\frac{x}{1-z}, Q^2\Big)$ can

be written as

$$G\Big(\frac{x}{1-z},Q^2\Big)\Big|_{z=\frac{1}{2}} = G\Big(z=\frac{1}{2},Q^2\Big)+\Big(z-\frac{1}{2}\Big)\frac{\partial G\Big(z=\frac{1}{2},Q^2\Big)}{\partial x}$$
$$= G(2x,Q^2)+\Big(z-\frac{1}{2}\Big)\frac{\partial G(2x,Q^2)}{\partial x}. \quad (4.6)$$

Using equation (4.6) and leading order terms of equation (4.4) in equation (4.5) and performing the integration, we get

$$F_L^g(x,Q^2) =< e^2 > \frac{\alpha_s(Q^2)}{4\pi}P(x)G\Big(2x+\frac{Q(x)}{P(x)},Q^2\Big), \quad (4.7)$$

where

$$P(x)=\int_0^{1-x}\frac{dz}{1-z}\Big(C_{L,g}^1(1-z)\Big) \quad (4.8)$$

and

$$Q(x)=\int_0^{1-x}\frac{dz}{1-z}\Big(z-\frac{1}{2}\Big)\Big(C_{L,g}^1(1-z)\Big). \quad (4.9)$$

This result shows that the longitudinal structure function $F_L^g(x,Q^2)$ can be calculated using the low x gluon density from Donnachie Landshoff (DL) model [7] at LO. Similarly, when gluon density is expanded at $z=0.8$, the corresponding LO expression takes the form

$$F_L^g(x,Q^2) =< e^2 > \frac{\alpha_s(Q^2)}{4\pi}P(x)G\Big(5x+\frac{R(x)}{P(x)},Q^2\Big), \quad (4.10)$$

where

$$R(x)=\int_0^{1-x}\frac{dz}{1-z}(z-0.8)\Big(C_{L,g}^1(1-z)\Big). \quad (4.11)$$

Both the equations (4.7) and (4.10) show the behaviour of $F_L^g(x,Q^2)$ with respect to x. We have also checked this for $z=0.6,0.7,0.9$; but the best result is obtained in the

case of the expansion point of the gluon density at $z = 0.8$ in LO analysis, which is depicted in figure 4.1 in comparison with the experimental data and model fit.

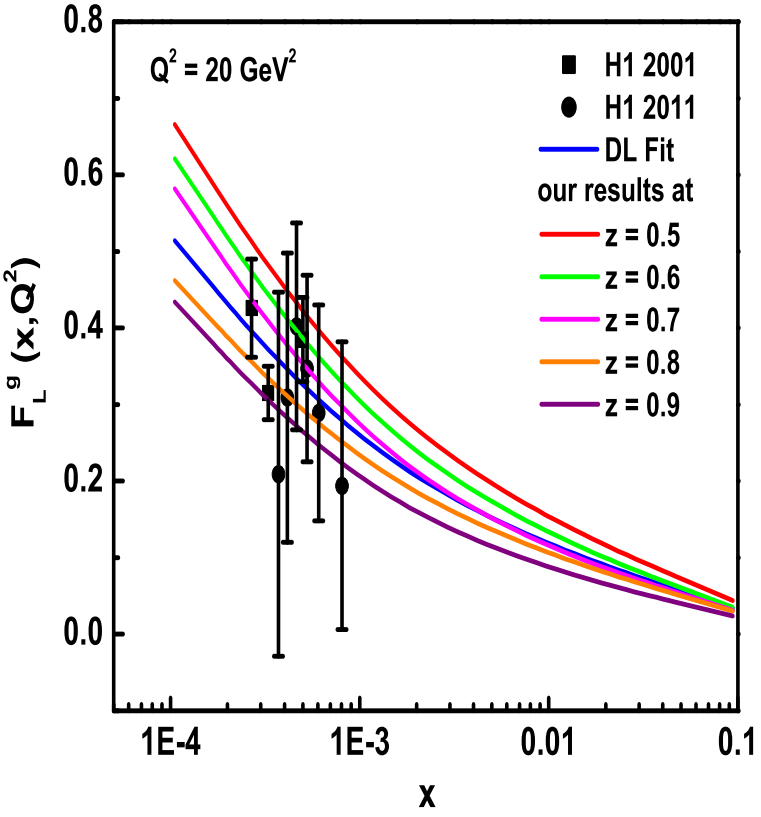

Figure 4.1: Sensitivity of our results of F_L^g structure function in LO with respect to the expansion point of gluon density at z = 0.5, 0.6, 0.7, 0.8, 0.9 in comparison with H1 data and DL model.

We have also obtained the relation between the longitudinal structure function and the gluon distribution function at small-x in NLO and NNLO analysis by considering the expansion point of the gluon density at $z = 0.8$. These are given by

$$F_L^g(x,Q^2) =< e^2 > \frac{\alpha_s(Q^2)}{4\pi} P_1(x) G\Big(5x + \frac{R_1(x)}{P_1(x)}, Q^2\Big) \tag{4.12}$$

and

$$F_L^g(x,Q^2) =< e^2 > \frac{\alpha_s(Q^2)}{4\pi} P_2(x) G\Big(5x + \frac{R_2(x)}{P_2(x)}, Q^2\Big) \tag{4.13}$$

in NLO and NNLO respectively. Here

$$P_1(x) = \int_0^{1-x} \frac{dz}{1-z}\Big(C_{L,g}^1(1-z) + T_0 C_{L,g}^2(1-z)\Big), \tag{4.14}$$

$$P_2(x) = \int_0^{1-x} \frac{dz}{1-z}\Big(C_{L,g}^1(1-z) + T_0 C_{L,g}^2(1-z) + T_1 C_{L,g}^3(1-z)\Big), \tag{4.15}$$

$$R_1(x) = \int_0^{1-x} \frac{dz}{1-z}(z-0.8)\Big(C_{L,g}^1(1-z) + T_0 C_{L,g}^2(1-z)\Big) \tag{4.16}$$

and

$$R_2(x) = \int_0^{1-x} \frac{dz}{1-z}(z-0.8)\Big(C_{L,g}^1(1-z) + T_0 C_{L,g}^2(1-z) + T_1 C_{L,g}^3(1-z)\Big). \tag{4.17}$$

Here we consider two numerical parameters T_0 and T_1, such that $T^2(t) = T_0.T(t)$ and $T^3(t) = T_1.T(t)$ with $T(t) = \frac{\alpha_s(t)}{2\pi}$. These numerical parameters are obtained for a particular range of Q^2 under study. As described in chapter 2 and ref. [20], these two parameters are chosen in such a way that the difference between $T^2(t)$, $T_0.T(t)$ and $T^3(t)$, $T_1.T(t)$ are negligible in our required range. Here, we have considered the values of $T_0 = 0.0278$ and $T_1 = 0.000892$ within the range $1.5 \leq Q^2 \leq 200GeV^2$. We have also checked the sensitivity of our results of F_L^g structure function in NLO and NNLO with respect to the expansion point of the gluon density at $z = 0.5, 0.6, 0.7, 0.8, 0.9$ which is depicted in figure 4.2. This figure shows that in case of the expansion point of gluon density at $z = 0.8$, our results show better agreement with the results of model fit and experimental data. Therefore, in all the cases of our calculated results of F_L^g structure function, i.e., in LO, NLO and NNLO analysis, the results calculated with respect to

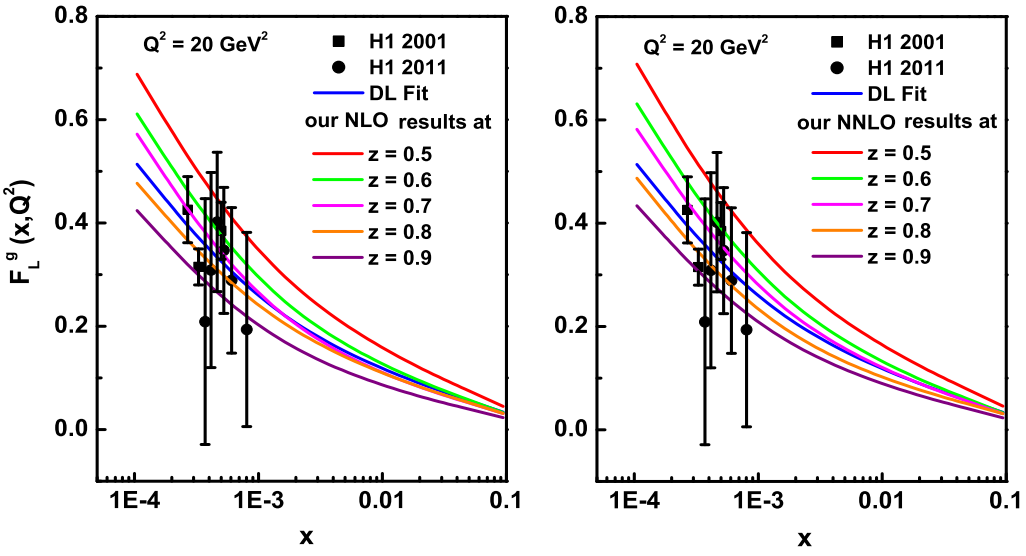

Figure 4.2: Sensitivity of our results of F_L^g structure function in NLO and NNLO with respect to the expansion point of gluon density at z = 0.5, 0.6, 0.7, 0.8, 0.9 in comparison with H1 data and DL model.

the expansion point of the gluon density at $z = 0.8$ shows compatibility with the results of model fit and data. In a similar way we have also checked the sensitivity of z values for all values of Q^2 like the values of $Q^2 = 20GeV^2$ which is found to be 0.8.

Thus using equations (4.10), (4.12) and (4.13) we have calculated the x-evolutions for F_L^g structure function in LO, NLO and NNLO respectively.

4.2 Results and Discussions

We have determined the approximate relation between the longitudinal structure function of proton and gluon distribution function at small-x in next-next-to-leading order analysis with respect to the expansion of the gluon density at an arbitrary point of expansion. With the help of these relations we have calculated the F_L^g structure

function in the range $10^{-4} \leq x \leq 0.1$ and $15 \leq Q^2 \leq 200GeV^2$ using the small-x gluon distribution function of DL model and the co-efficient functions which are given in Appendix A. The obtained results are compared with the the recent H1 [1–5], ZEUS [6] experimental data and results of DL model [7]. The related plots are depicted in figure 4.3 which indicate a good agreement with experimental data and model fit. Here, the vertical error bars are both statistical and systematic errors for both H1 and ZEUS data. To confirm that in spite of the large uncertainty in the experimental data, our results are in good agreement with the other results, we also add DL model results. We have also compared our results with the theoretical predictions of MSTW08 [8], CT10 [9,10], ABM11 [11] and NNPDF2.3 [12, 13] parameterizations. Figures 4.4 to 4.7 show the related plots for different values of $Q^2 = 20, 25, 80$ and $200GeV^2$. These plots also reflect better agreement of our results with these parameterizations. Here all the plots show compatibility with predictions of parameterizations towards higher values of Q^2 i.e., $Q^2 = 80$ and $200GeV^2$. In this procedure of evaluation of F_L^g structure function as we have taken the input distribution of gluon from DL model, so the behaviour of structure function increases towards small-x depending on values of the input distribution. Our calculated results of F_L^g structure function in all the cases i.e., LO, NLO and NNLO increases towards small values of x in the given range of x and Q^2 as expected from QCD.

In our analysis, we have determined the approximate relation between F_L^g structure function of proton and gluon distribution function at small-x in next-next-to-leading order using the Altarelli- Martinelli equation for F_L^g structure function in terms of the co-efficient functions. We have also compared our results at moderate values of $Q^2 = 20GeV^2$ with the similar results obtained by Sarkar et al (CS) [17] and Boroun et al (GRB) [21]. In ref. [17], the authors suggested a relation between F_L structure function of proton and gluon distribution function at small-x in leading order approximation

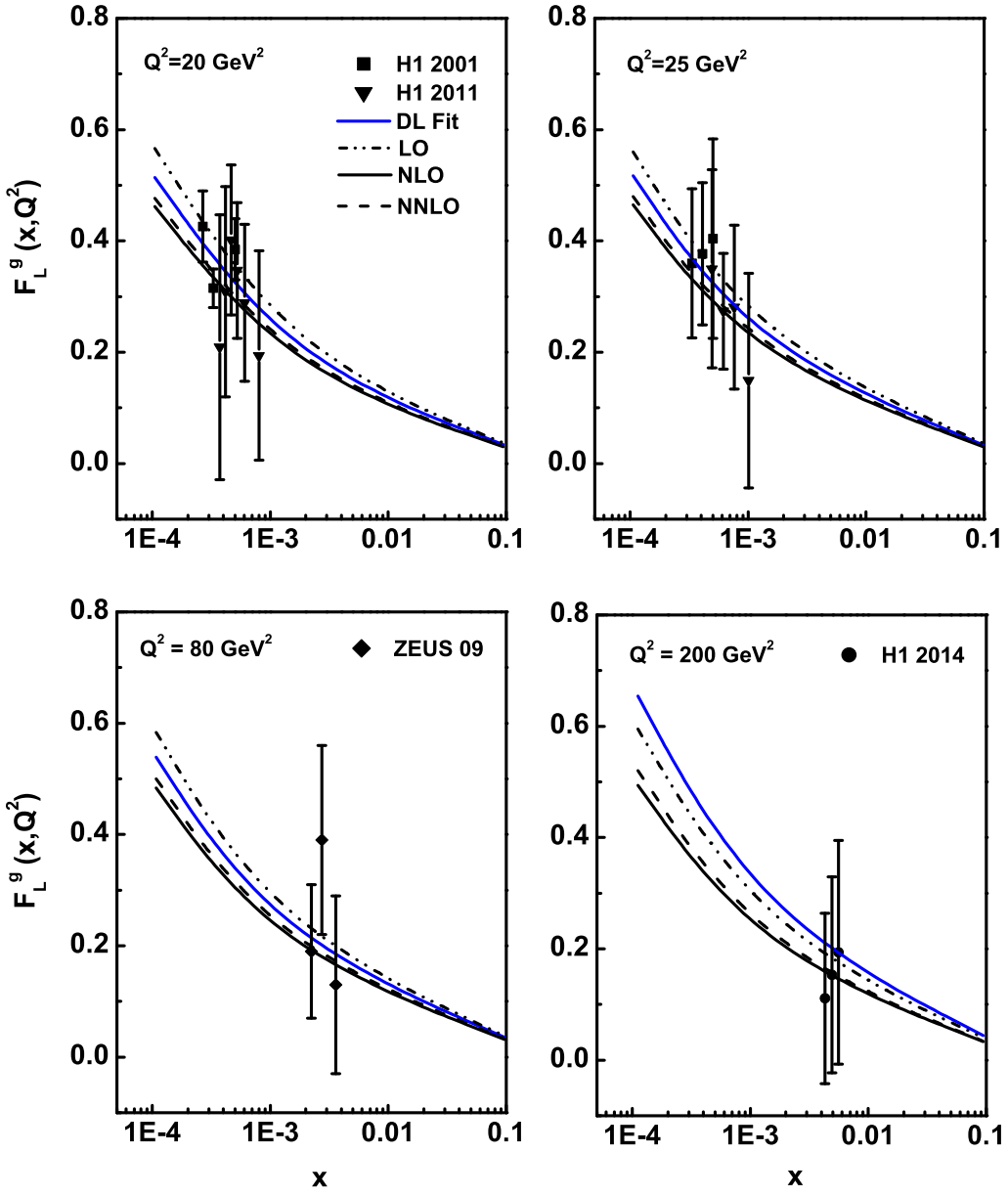

Figure 4.3: x-evolution results of F_L^g structure function up to NNLO using Taylor expansion method in comparison with the H1, ZEUS data and results of DL model.

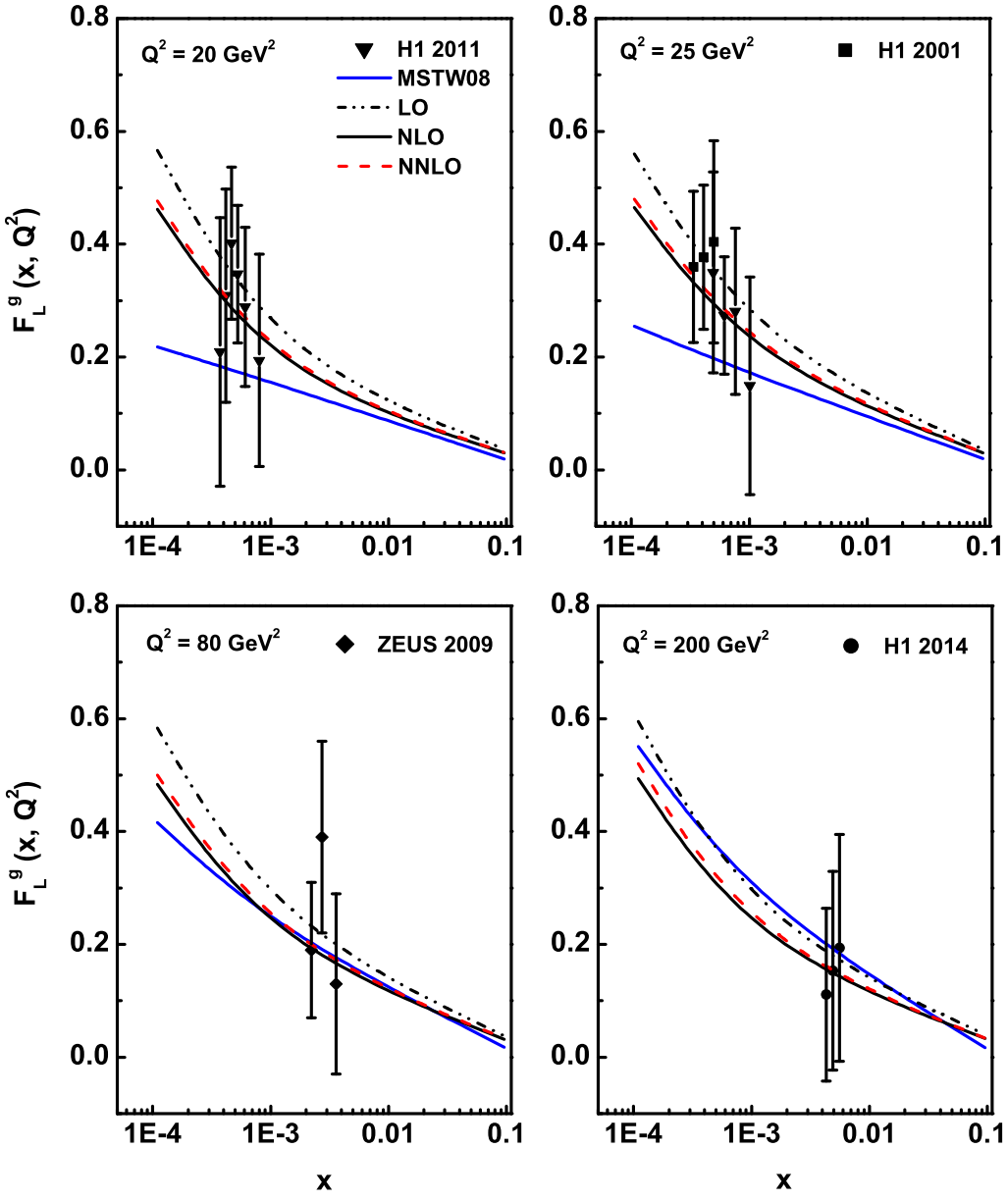

Figure 4.4: x-evolution results of F_L^g structure function up to NNLO using Taylor expansion method in comparison with the H1, ZEUS data and the theoretical prediction of MSTW08.

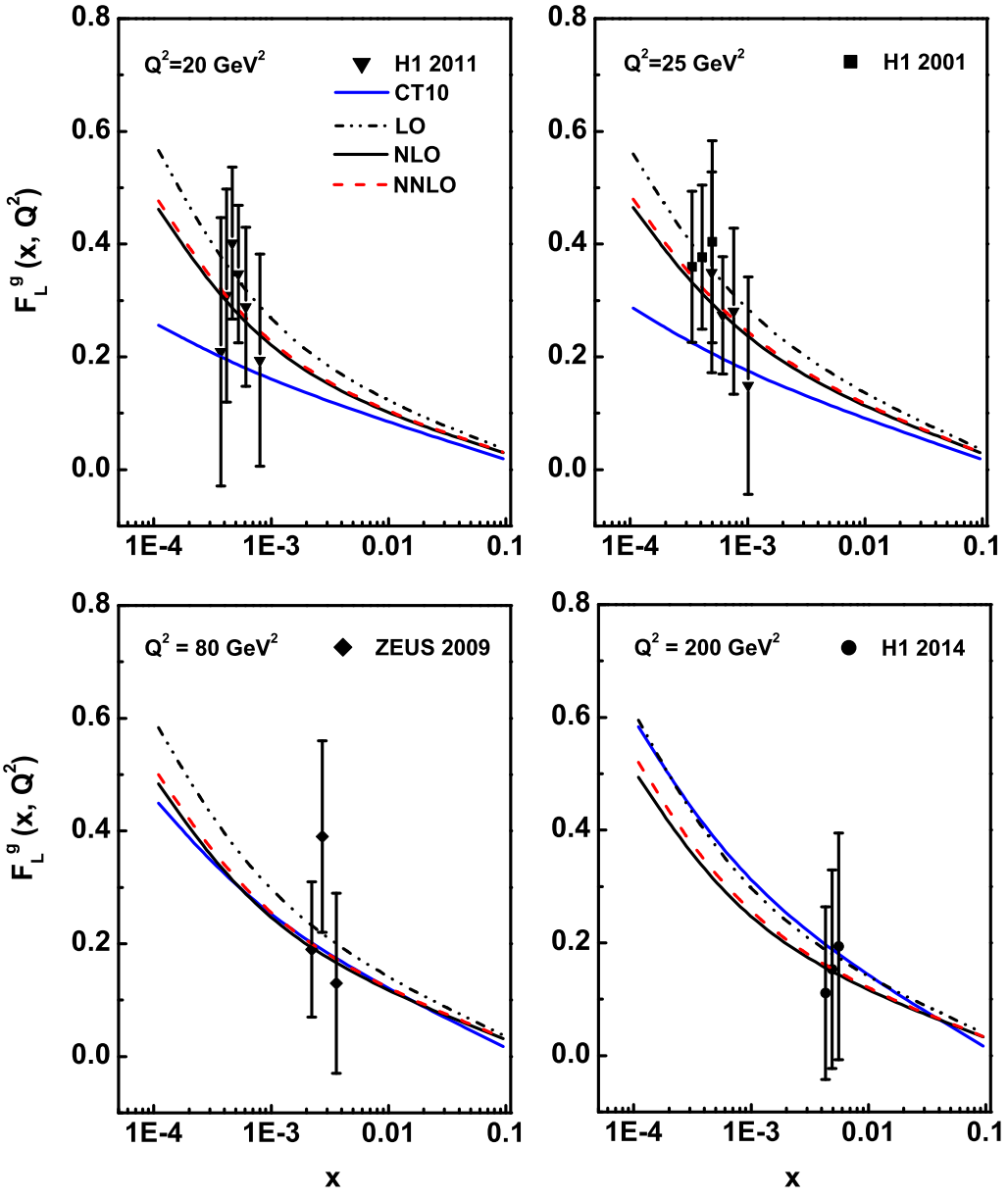

Figure 4.5: x-evolution results of F_L^g structure function up to NNLO using Taylor expansion method in comparison with the H1, ZEUS data and the theoretical prediction of CT10.

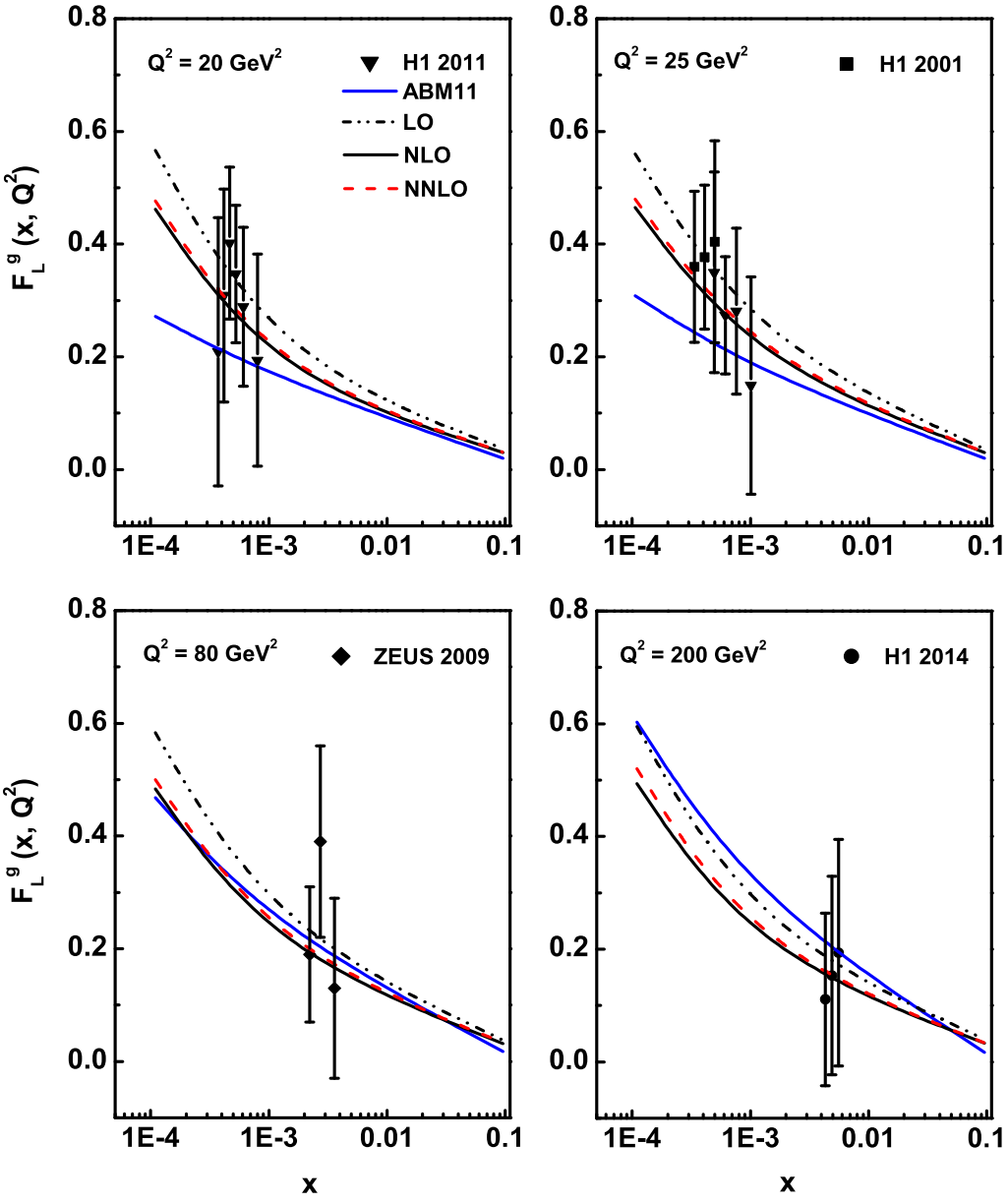

Figure 4.6: x-evolution results of F_L^g structure function up to NNLO using Taylor expansion method in comparison with the H1, ZEUS data and the theoretical prediction of ABM11.

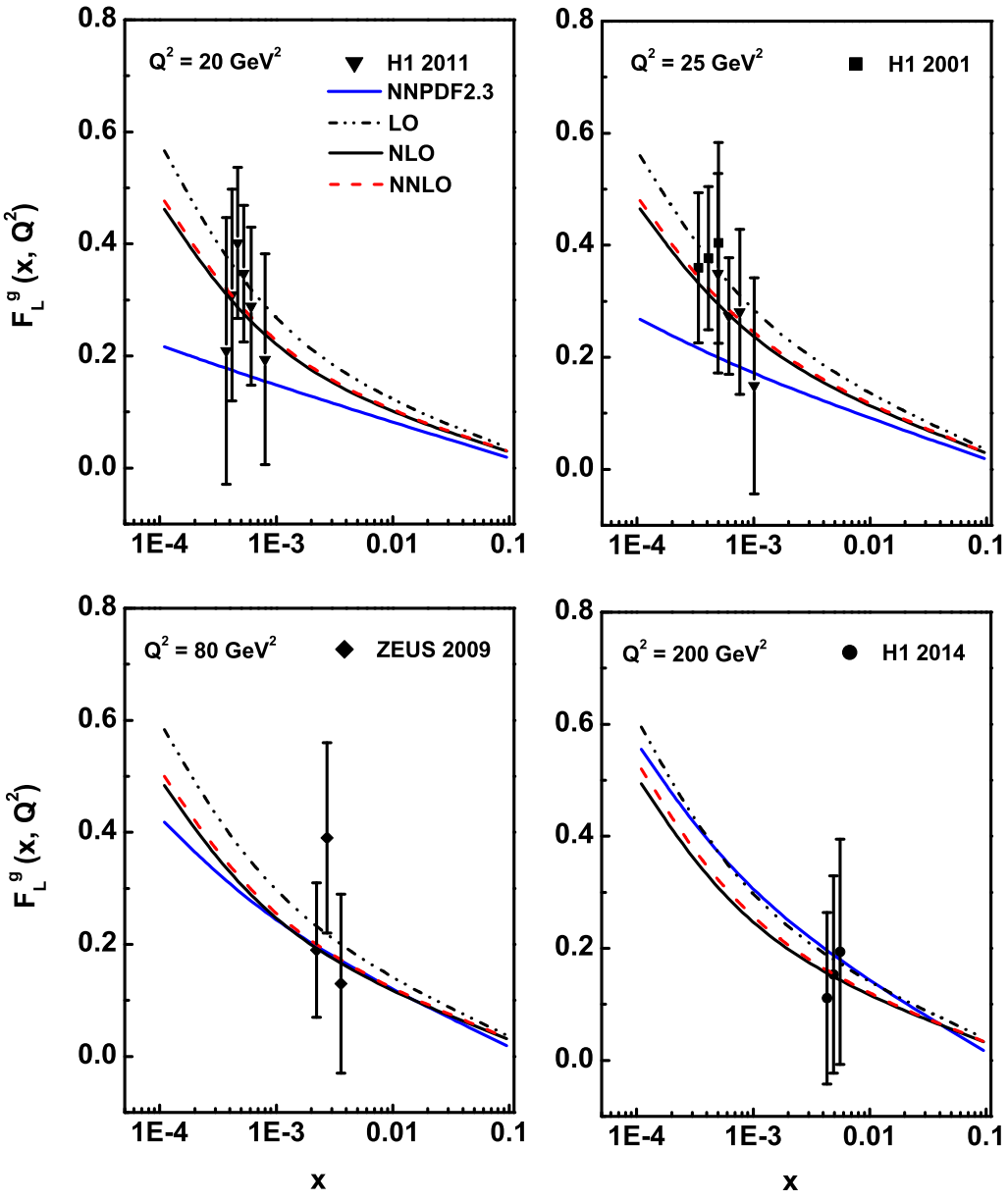

Figure 4.7: x-evolution results of F_L^g structure function up to NNLO using Taylor expansion method in comparison with the H1, ZEUS data and the theoretical prediction of NNPDF2.3.

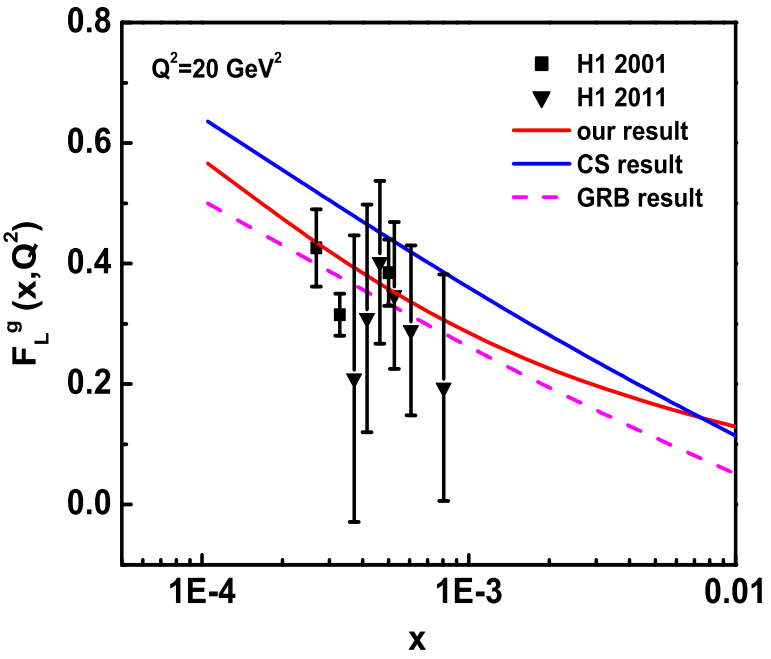

Figure 4.8: comparison of our x-evolution results of F_L^g structure function with the results of Sarkar et al (CS) and Boroun et al (GRB).

given by

$$F_L^g(x,Q^2) = \frac{2\alpha_s}{\pi}\frac{\sum_{i=1}^{N_f} e_i^2}{5.9} G(2.5x,Q^2) \tag{4.18}$$

which shows the close relation between these two quantities. In ref. [21], the authors reported an NLO analysis of the relation between F_L structure function and gluon distribution obtained by Sarkar et al. Figure 4.8 shows the comparison of our results with the above mentioned two results which reflects similar behaviour with the results obtained by Sarkar et al (CS) and Boroun et al (GRB). Thus our approximate relation can be used to study the x-evolution of F_L^g structure function at small-x up to NNLO analysis.

4.3 Conclusions

In this work, we have determined the proton longitudinal structure function up to NNLO at small-x using the approximate relation between F_L^g structure function and gluon distribution function with respect to the expansion of the gluon density at an arbitrary point of expansion i.e., at $z = 0.8$. The behaviour of F_L^g structure function with x shows good agreement with the experimental data and the model fit and parameterizations. Our predicted results also shows resemblance with the results obtained by other authors. The calculated results of F_L^g structure function in all orders lies within the framework of pQCD i.e, it increases towards low values of x. As at small-x gluon contents in the proton is dominant one we can say that gluon contribution to the F_L structure function increases as x decreases.

References

[1] Aaron, F. D., et al. Measurement of the inclusive $e^{\pm}p$ scattering cross section at high inelasticity y and of the structure function F_L, *Eur. Phys. J. C.* **71** (3), 1579-1–50, 2011.

[2] Adloff, C., et al. Deep-inelastic inclusive ep scattering at low x and a determination of α_s, *Eur. Phys. J. C.* **21** (1), 33–61, 2001.

[3] Pardos, C. D. *Studies for the direct measurement of the proton structure function F_L with the H1 detector at HERA*, Ph.D. thesis, DESY, Zeuthen, Germany, 2007.

[4] Piec, S. *Measurement of the Proton Structure Function F_L with the H1 Detector at HERA*, Ph.D. thesis, Humboldt University of Berlin, Germany, 2009.

[5] Andreev, V., et al. Measurement of Inclusive *ep* Cross Sections at High Q^2 at $\sqrt{s} = 225$ and $252GeV$ and of the Longitudinal Proton Structure Function F_L at HERA, *Eur. Phys. J. C* **74** (4), 2814-1–26, 2014.

[6] Chekanov, S., et al. Measurement of the longitudinal proton structure function at HERA, *Phys. Lett. B* **682** (1), 8–22, 2009.

[7] Donnachie, A. and Landshoff, P. V. The protons gluon distribution, *Phys. Lett. B* **550** (3-4), 160–165, 2002.

[8] Martin, A. D., et al. Parton distributions for the LHC, *Eur. Phys. J. C* **63** (2), 189–285, 2009.

[9] Hung-Liang, Lai., et al. New parton distributions for collider physics, *Phys. Rev. D* **82** (7), 074024-1–24, 2010.

[10] Jun, Gao., et al. CT10 next-to-next-to-leading order global analysis of QCD, *Phys. Rev. D* **89** (3), 033009-1–28, 2014.

[11] Alekhin, S., Bluemlein, J. and Moch, S. The ABM parton distributions tuned to LHC data, *Phys. Rev. D* **89** (5), 054028-1–21, 2014.

[12] Ball, R. D., et al. Parton distributions with LHC data, *Nucl. Phys. B* **867** (2), 244–289, 2013.

[13] Forte, S., et al. Heavy quarks in deep-inelastic scattering, *Nucl. Phys. B* **834** (1-2), 116–162, 2010.

[14] Altarelli, G. and Martinelli, G. Transverse momentum of jets in electroproduction from quantum chromodynamics, *Phys. Lett. B* **76** (1), 89–94, 1978.

[15] Moch, S., Vermaseren, J. A. M. and Vogt, A. The longitudinal structure function at the third order, *Phys. Lett. B* **606** (1-2), 123–129, 2005.

[16] Abbott, L. F., Atwood, W. B. and Barnett, R. M. Quantum-chromodynamic analysis of eN deep-inelastic scattering data, *Phys. Rev. D* **22** (3), 582–593, 1980.

[17] Cooper-Sarkar, A. M., et al. Measurement of the longitudinal structure function and the small x gluon density of the proton, *Z. Phys. C* **39** (2), 281–290, 1988.

[18] Zijlstra, E. B. and Van Neerven, W. L. Contribution of the second order gluonic Wilson coefficient to the deep inelastic structure function, *Phys. Lett. B* **273** (4), 476–482, 1991.

[19] Moch, S. and Vermaseren, J. A. M. Deep-inelastic structure functions at two loops, *Nucl. Phys. B* **573** (3), 853–907, 2000.

[20] Baishya, R. and Sarma, J. K. Semi numerical solution of non-singlet Dokshitzer-GribovLipatovAltarelliParisi evolution equation up to next-to-next-to-leading order at small x, *Eur. Phys. J. C* **60** (4), 585–591, 2009.

[21] Boroun, G. R. and Rezaei, B. Analysis of the proton longitudinal structure function from the gluon distribution function, *Eur. Phys. J. C* **72** (11), 2221-1–5, 2012. □